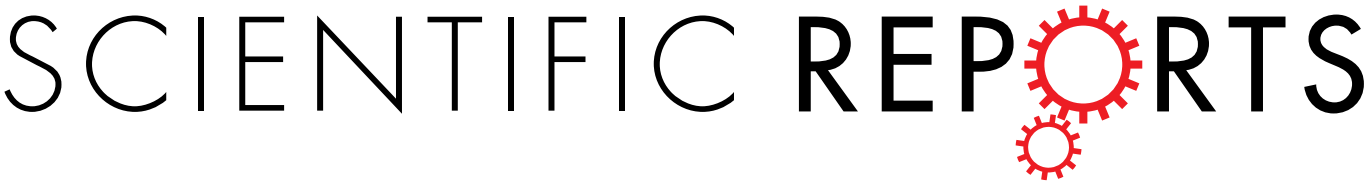

OPEN

Room temperature three-photon pumped $CH_3NH_3PbBr_3$ perovskite microlasers

Received: 06 December 2016
Accepted: 27 February 2017
Published: 28 March 2017

Yisheng Gao[1], Shuai Wang[1], Can Huang[1], Ningbo Yi[1], Kaiyang Wang[1], Shumin Xiao[1,2] & Qinghai Song[1,2]

Hybrid lead halide perovskites have made great strides in next-generation light-harvesting and light emitting devices. Recently, they have also shown great potentials in nonlinear optical materials. Two-photon absorption and two-photon light emission have been thoroughly studied in past two years. However, the three-photon processes are rarely explored, especially for the laser emissions. Here we synthesized high quality $CH_3NH_3PbBr_3$ perovskite microstructures with solution processed precipitation method and studied their optical properties. When the microstructures are pumped with intense 1240 nm lasers, we have observed clear optical limit effect and the band-to-band photoluminescence at 540 nm. By increasing the pumping density, whispering-gallery-mode based microlasers have been achieved from $CH_3NH_3PbBr_3$ perovskite microplate and microrod for the first time. This work demonstrates the potentials of hybrid lead halide perovskites in nonlinear photonic devices.

Hybrid lead halide perovskites have been intensively studied due to their potential applications in photovoltaic devices[1–3]. In just four years, the light conversion coefficient has been dramatically improved from 3.5%[4] to more than 22.1%[5], which is comparable to or even larger than most of the thin film solar cells. In principle, the ferroelectric nature of hybrid lead halide perovskite has been considered to play an essential role in photovoltaic performances[6,7]. The ferroelectric domains help the separation of photo-excited electron and hole pairs, and the reduction of recombination through segregation of charge carriers[6]. The ferroelectric character can also induce quantum coherent wave propagation of exciton, which leads to more efficient charge extraction[7]. Interestingly, such kind of ferroelectric properties of hybrid lead halide perovskites also make them to be comparable to the other ferroelectric materials such as lithium niobate[8–12]. Consequently, the nonlinear optical properties can be expected in the hybrid lead halide perovskites. Within past two years, a number of nonlinear effects have been experimentally demonstrated, e.g. two-photon absorption[8–10], two-photon pumped photoluminescence (PL)[8], two-photon pumped amplified spontaneous emission (ASE)[13], and two-photon pumped lasers[14]. Very recently, three-photon pumped PL and amplifications have also been reported[15]. However, compared with the two-photon process, the three-photon absorption and three-photon emission are higher order nonlinear process and have much smaller coefficients/cross sections. Till now, only the three-photon ASE has been observed in hybrid lead halide perovskite bulk[15]. Three-photon excited lasers are still absent, especially in the hybrid lead halide microstructures. Therefore, considering the progresses in water-resistant perovskite[16–18], it is also very essential and highly desirable to develop a three-photon pumped hybrid lead halide perovskite microlasers at room-temperature. Here we have synthesized single-crystalline $CH_3NH_3PbBr_3$ microstructures and demonstrated the three-photon excited lasing actions within them for the first time.

Results and Discussion

Figure 1(a) shows the top-view scanning electron microscope (SEM) image of the synthesized microstructures. We can see that the synthesized microstructures are dominated by the microplates and microrods. The lengths of these microstructures are tens of microns. The widths of the microrods vary between a few to several microns. The thicknesses of two types of microstructures are quite different. The thicknesses of microplates are usually

[1]State Key Laboratory on Tunable laser Technology, Ministry of Industry and Information Technology Key Lab of Micro-Nano Optoelectronic Information System, Shenzhen Graduate School, Harbin Institute of Technology, Shenzhen, 518055, China. [2]Collaborative Innovation Center of Extreme Optics, Shanxi University, Taiyuan, 030006, China. Correspondence and requests for materials should be addressed to S.X. (email: shumin.xiao@hitsz.edu.cn) or Q.S. (email: qinghai.song@hitsz.edu.cn)

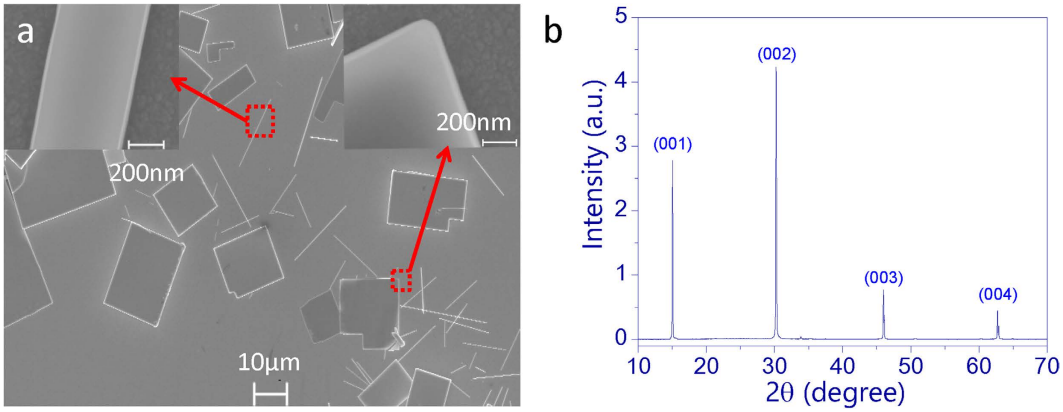

Figure 1. (**a**) Top-view SEM image of the synthesized microstructures. The insets show the high resolution SEM images of microplate and microrod. (**b**) XRD spectrum of $CH_3NH_3PbBr_3$ microstructures.

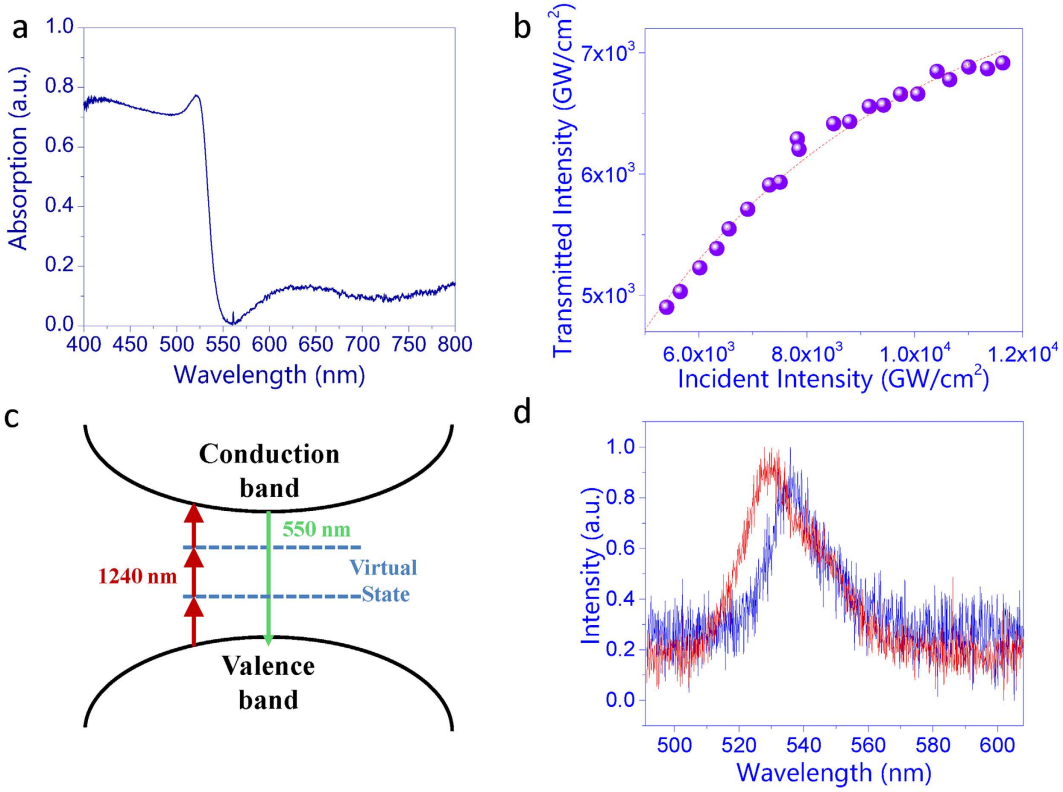

Figure 2. (**a**) Linear absorption of the $CH_3NH_3PbBr_3$ microstructures. (**b**) The transmission of an ultrashort pulse at 1240 nm as a function of incident power. The dashed line represent the fitted curve following equation (2). (**c**) The schematic pictures of the three-photon absorption. (**d**) The PL spectra under one-photon and three-photon excitations.

around several hundred nanometers to a few microns (see examples in Figure S4 in supplemental information). Figure 1(b) shows the recorded X-ray diffraction (XRD) spectrum of the synthesized microstructures. Sharp peaks can be clearly seen at around 15° and 30°, matching the cubic phase and indicating the single crystal very well. The insets in Fig. 1(a) are the high resolution top-view SEM images of a microplate and a microrod. We can see that the boundaries of perovskite microplate and microrod are extremely smooth and uniform. It is hard to see clear flaws and fluctuations even though the scar bar is already as small as 200 nm. Thus we know that the scattering loss at the side-facets are negligibly small and lasing actions are possibly formed within these high quality perovskite microstructures[19].

Then the optical properties of synthesized microstructures were studied. Figure 2(a) shows the regular absorption spectrum that was recorded by measuring the linear transmission and refection spectra with a continue-wave white light source (see Figure S1 in supplemental information). We can see that the absorption drastically

increases when the wavelength is below 550 nm (2.25 eV). For the wavelength range above 550 nm, the linearly material absorption is negligibly small. All these experimental observations are consistent with the previous reports very well[13,14,20]. The situation changed dramatically when the sample was illuminated with ultrashort laser pulses (100 fs, 1 KHz, see Figure S2 in supplemental information). One example is illustrated in Fig. 2(b), where the pumping wavelength is 1240 nm (1 eV). The transmitted energy increased linearly at low pumping density. With the increase of pumping power, the transmitted energy gradually deviated from the linear model (dashed line in Fig. 2(b)) and an obvious transmission limit can be observed. All these experimental results clearly indicate the occurrence of nonlinear absorption. Since the photon energy of pumping laser is smaller than half of the bandgap (2.25 eV) and larger than 1/3 of the bandgap, here the nonlinear absorption is induced by the three-photon process (see the corresponding schematic picture in Fig. 2(c)).

According to the basic theoretical consideration of three-photon, the intensity change of an excitation beam along the propagation direction (x direction) can be expressed as[21]

$$\frac{dI(x)}{dx} = -\gamma I^3(x), \tag{1}$$

where γ is the three-photon-absorption coefficient of $CH_3NH_3PbBr_3$ microplate. The solution of equation (1) can thus be obtained as

$$\mathrm{I}(x) = \frac{I_0}{\sqrt{1 + 2\gamma x I_0^2}} \tag{2}$$

Therefore, the three-photon-absorption coefficient $\gamma = 2.26 \times 10^{-5} cm^3/GW^2$ have been obtained by fitting the data in Fig. 2(b).

The existence of three-photon absorption can also be confirmed from the emissions of the nanostructures. When the microstructures were excited with an ultrashort pulsed laser at 1240 nm, green light has been clearly observed (see the optical setup in Figure S3 supplemental information). Figure 2(d) shows the PL spectra under three-photon excitations. We can see that the central wavelength slightly shifts to longer wavelength about 10 nm and the full width at half maximum (FWHM) decreases from ~30 nm to ~20 nm. Similar to the two-photon process, both of the redshift and decrease in FWHM are also caused by the re-absorption of three-photon emission in hybrid halide perovskites[22].

Based on the information on three-photon absorption and PL, the three-photon excited lasing action has been studied in one hybrid lead halide perovskite based microplate. The corresponding top-view SEM image is shown in Fig. 3(a). We can see that the microplate has a rectangle shape. The length and width of the rectangle are 65.4 microns and 39.2 microns, respectively. The thickness, which is measured by alfa stepper, is 1600 nm (see Figure S4 in supplemental information). When the pumping density was low, the emission spectrum was a broad spontaneous emission peak, which was similar to the one in Fig. 2(d). In the log-log plot, the integrated output intensity increases linearly with the pumping density. As shown in Fig. 3(c), the power slope of fitting line is 3.1, which is another direct evidence for the existence of three-photon absorption and PL[15,21]. Once the pumping power was above 170 mJ/cm^2, the power slope drastically increases from around 3.3 to around 12.3. Meanwhile, sharp laser peaks emerged and quickly dominated the emission spectrum (see Fig. 3b). The emergence of sharp peaks and the changes in power slope clearly confirmed the three-photon pumped lasing action in $CH_3NH_3PbBr_3$ microplate[23–25]. While the three-photon ASE has been reported in $CH_3NH_3PbI_3$ bulk[15], this is the first time that three-photon excited micro-lasers have been demonstrated, especially at the room temperature.

Figure 3(b) depicts the spectrum of three-photon laser emissions from the $CH_3NH_3PbBr_3$ microplate. We can see a series of periodic peaks in the laser spectrum. The recorded mode spacing is 0.68 nm. The inset in Fig. 3(b) shows the corresponding fluorescent microscope image. With the onset of three-photon lasers, bright spots have also been seen at two end-facets of the short side. Based on the previous reports, it is easy to know that the three-photon lasers are generated along the short side. The polarization of emitted lasers were also recorded and plotted as inset in Fig. 3(c). The main polarization is along the long side of microplate. Thus we know that the transverse electric (TE, E is in-plane) polarized lasers have been formed.

As the conventional microlasers are one-to-one correspondence with the resonant modes, we thus numerically calculated the eigenmodes inside the microplate to understand the experimental observations. All the numerical calculations were performed with a finite element method based software package (Comsol Multiphysics 3.5a). Because the lasers were formed within the pumped strip along the short side, the system can be simplified into a two-dimensional rectangle in the transverse plane (see the details in Figure S5 in supplemental information)[26,27]. Figure 3(d) shows the numerically calculated quality (Q) factors of resonances inside the cavity. Here the cavity structures and refractive index were all taken from experimental data and material dispersions have been considered[28]. Due to the relative large refractive index of hybrid lead halide perovskite, the cavity can support a number of resonant modes. Around the lasing wavelength, a number of resonant modes marked 1–5 have relatively high Q factors and are easily excited in optical experiment. The mode spacing of modes 1–5 are around 0.65 nm, which is very close to the experimental result. Thus we know that the resonances 1–5 correspond to the lasing modes well. The inset in Fig. 3(d) shows the field pattern of resonance 2. Different from the conventional Fabry-Perot modes, we find that the light has an incident angle around 45 degree on two end-facets. Considering the large refractive index, the light is totally reflected and the resonances are whispering gallery like modes. For such kind of rectangle resonator, the main leakages are the boundary wave leakage and the pesudointegrable leakage[29–31].

In additional to the three-photon lasers in $CH_3NH_3PbBr_3$ microplates, we have also studied three-photon lasing action in $CH_3NH_3PbBr_3$ microrods. One example is summarized in Fig. 4. The top-view SEM image of the microrod is shown in Fig. 4(a). The length of microrod is 18.7 microns and its width is 1300 nm. The thickness

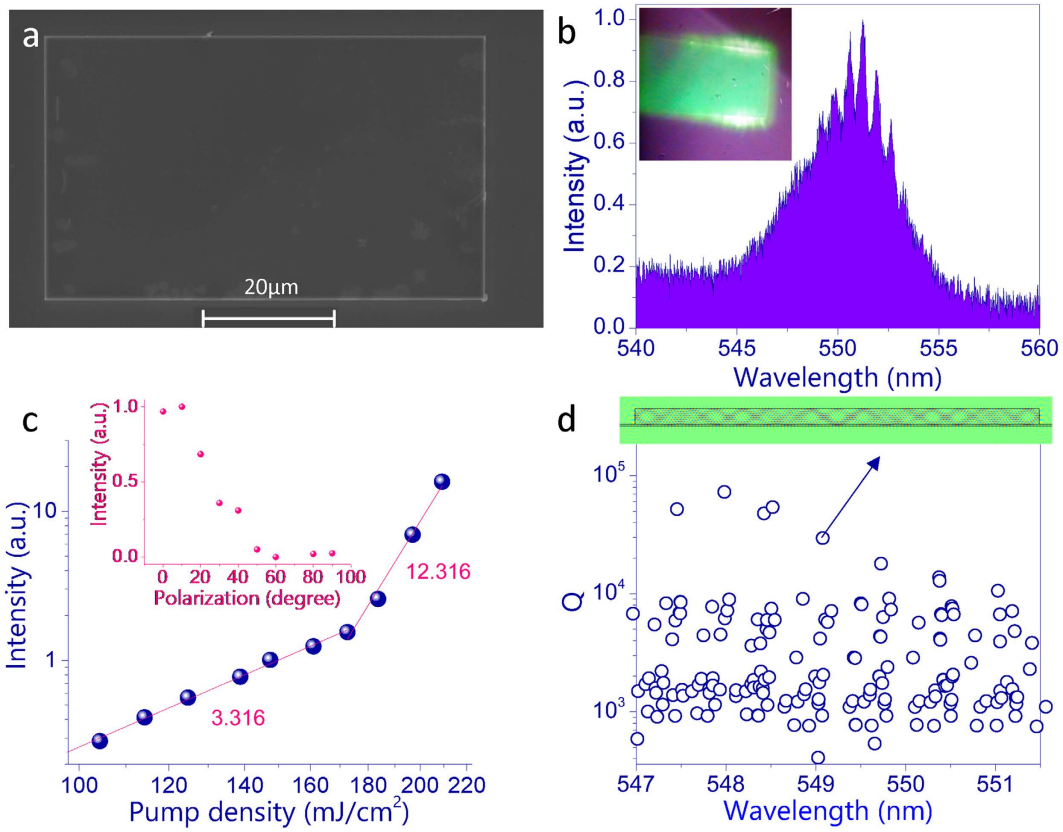

Figure 3. (**a**) Top view SEM image of a rectangle $CH_3NH_3PbBr_3$ microplate. (**b**) The emission spectrum of the microplate with the pumping density at 197 mJ/cm^2. The inset is the corresponding fluorescent microscope image. (**c**) The integrated output intensity as a function of pumping density. Inset shows the polarization of emitted laser in (**b**). (**d**) The numerical calculated cavity Q factors within the lasing wavelength range. The inset is the field pattern (Ez) of mode-1.

of microrod is around 835 nm, which is shown in Figure S4 in supplemental information. Figure 4(b) shows the three-photon emission spectra under different pumping conditions. When the pumping power was low, a broad PL peak was seen at 547 nm (see Fig. 2(d) as an example) with full width at half maximum around 20 nm. With the increase of pumping power to above 130 mJ/cm^2, periodic peaks appeared and quickly dominated the emission spectrum (see Fig. 4(b)). Figure 4(c) summarizes the output intensity as a function of pumping density. When the pumping power was low, the output intensity increased with a power slope ~3.3 in log-log plot, clearly demonstrating the three-photon PL process. When the pumping density was above 130 mJ/cm^2, a dramatic change in power slope was observed. Meanwhile, the full width at half maximum of emission spectrum decreases from ~20 nm to ~0.3 nm, giving a Q factor around 1800. As mentioned above, the dramatic change in power slope and linewidth clearly demonstrated the onset of three-photon pumped microlaser.

The inset in Fig. 4(c) shows the fluorescent microscope image of the microrod with pumping density of 138.5 mJ/cm^2. Similar to Fig. 3, bright spots can be observed at the end-facets of the $CH_3NH_3PbBr_3$ microrod. This image indicated that the lasers were formed along the axial direction of the microrod. This is different from the transverse mode in Fig. 3. Another difference lies in the polarization. As shown in Figure S6 in the supplemental information, the polarization of three-photon microrod laser is following the axial direction, demonstrating the transverse magnetic (TM) polarization well.

Based on above information, we have also numerically simulated the resonances inside the system. All the results are shown in Fig. 4(d). While a large number of resonances have been formed around lasing wavelength range, there are several modes have much higher Q factors and have similar mode spacing with the experimental results. The inset in Fig. 4(d) shows the field pattern (Ez) of the highest Q resonant mode. We can see that this mode is also confined by total internal reflection at two end-facets. Compared with the modes in Fig. 3(d), here mode coupling happens[30,31] and the field distributions are pushed away from the corners. Consequently, the boundary wave leakage is suppressed and the laser threshold in Fig. 4(c) was relatively lower than the one in Fig. 3(c).

Conclusion

In summary, we have studied the three-photon process in single crystal $CH_3NH_3PbBr_3$ microstructures. The measured three-photon-absorption coefficient was as large as. $\gamma = 2.26 \times 10^{-5} cm^3/GW^2$ Based on the large three-photon-absorption of hybrid lead halide perovskites, three-photon excited whispering-gallery-mode lasers have been experimentally observed in both of perovskite microplate and microrod for the first time. This research

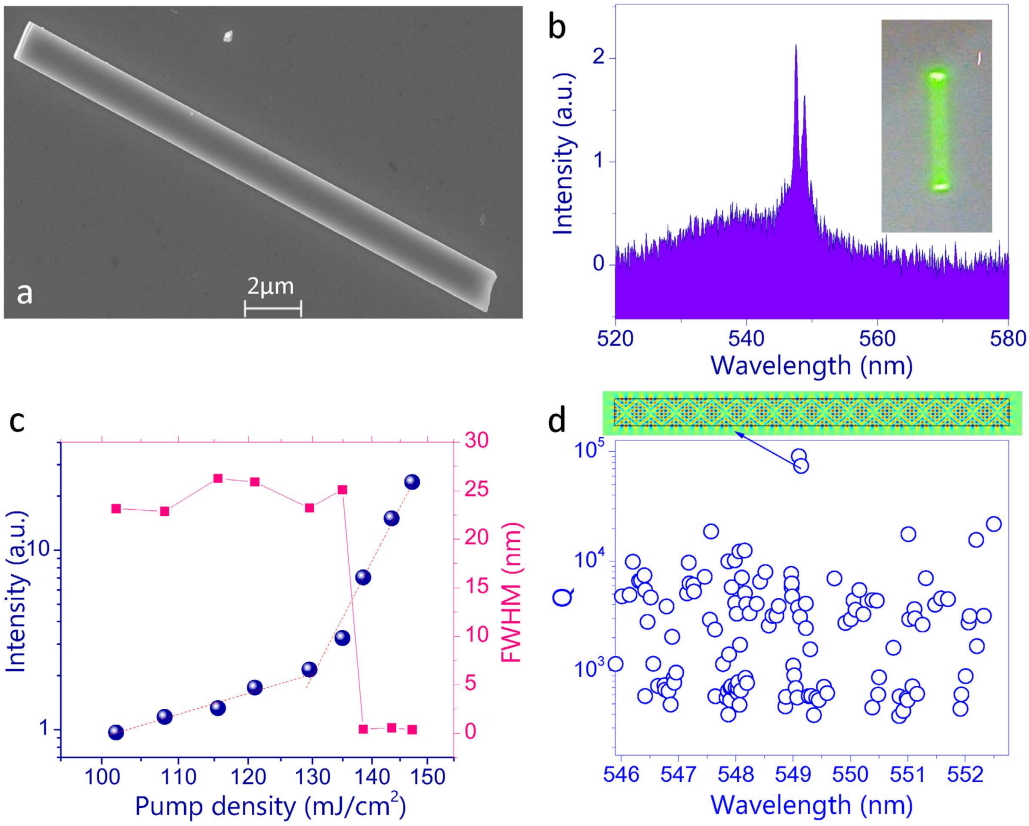

Figure 4. (**a**) Top view SEM image of a $CH_3NH_3PbBr_3$ microrod. (**b**) The emission spectrum of transverse lasing mode in the microrod with the pumping density at 138.5 mJ/cm^2. Inset shows the fluorescent microscope image. (**c**) The dependence of output intensity (dots) and the linewidth (squares) on the pumping density. (**d**) The numerical calculation results of resonant modes in microrod. Inset is the field pattern (Ez) of the highest Q mode.

shows that the hybrid lead halide perovskite has very large fifth-order nonlinearity, which will be essential for practical applications such as optical switch. Compared with the two-photon process, three-photon absorption, PL, and lasers have much longer pumping laser wavelengths and the pumping lasers can propagate longer in highly scattering medium or cells. Therefore, considering the rapid developments in water resist lead halide perovskite, this research will also be important for developing active devices.

Methods

Fabrication. We synthesized the single crystalline $CH_3NH_3PbBr_3$ microstructures with a solution based precipitation process[14,20]. Basically, CH_3NH_3Br (0.04 mmol) and $PbBr_2$ (0.04 mmol) were dissolved in N, N-dimethyformamide (DMF) at a concentration of 0.02 M independently. Two solutions were mixed at room temperature (humidity 50%) with a 1:1 volume ratio. And a CH_3NH_3Br•$PbBr_2$ solution with a concentration at 0.01 M has been formed. The diluted solution was dip-casted onto an ITO-coated glass substrate which was fixed at a teflon stage. Then the teflon stage was sealed in a beaker with Dichloromethane (DCM = CH_2Cl_2). After 36 h, hybrid lead halide perovskites ($CH_3NH_3PbBr_3$) microstructures were successfully synthesized on the substrate.

Simulation and Measurement. The simulation of microplate and microrod were calculated by COMSOL MULTIPHYSICS and the experiment results were measured using an analog microscope system built by ourselves. The details of simulation and measurements are showed in support information.

References

1. Green, M. A., Ho-Baillie, A. & Snaith, H. J. The emergence of perovskite solar cells. *Nature Photonics* **8,** 506–514, doi: 10.1038/nphoton.2014.134 (2014).
2. Yuan, M. *et al.* Perovskite energy funnels for efficient light-emitting diodes. *Nature nanotechnology* **11,** 872–877, doi: 10.1038/nnano.2016.110 (2016).
3. Snaith, H. J. Perovskites: The Emergence of a New Era for Low-Cost, High-Efficiency Solar Cells. *Journal of Physical Chemistry Letters* **4,** 3623–3630, doi: 10.1021/jz4020162 (2013).
4. Kojima, A., Teshima, K., Shirai, Y. & Miyasaka, T. Organometal Halide Perovskites as Visible-Light Sensitizers for Photovoltaic Cells. *Journal of the American Chemical Society* **131,** 6050−+, doi: 10.1021/ja809598r (2009).
5. Wilson G. & Hulstrom R. Research Cell Efficiency Records. http://www. nrel. gov/ncpv/images/efficiency_chart. jpg (2012).
6. Frost, J. M. *et al.* Atomistic origins of high-performance in hybrid halide perovskite solar cells. *Nano letters* **14,** 2584–2590, doi: 10.1021/nl500390f (2014).
7. Grinberg, I. *et al.* Perovskite oxides for visible-light-absorbing ferroelectric and photovoltaic materials. *Nature* **503,** 509–512, doi: 10.1038/nature12622 (2013).

8. Walters, G. *et al.* Two-Photon Absorption in Organometallic Bromide Perovskites. *ACS nano* **9,** 9340–9346, doi: 10.1021/acsnano.5b03308 (2015).
9. Kalanoor, B. S. *et al.* Third-Order Optical Nonlinearities in Organometallic Methylammonium Lead Iodide Perovskite Thin Films. *ACS Photonics* **3,** 361–370, doi: 10.1021/acsphotonics.5b00746 (2016).
10. Zhang, R. *et al.* Nonlinear Optical Response of Organic–Inorganic Halide Perovskites. *ACS Photonics* **3,** 371–377, doi: 10.1021/acsphotonics.5b00563 (2016).
11. Wang, Y. *et al.* All-Inorganic Colloidal Perovskite Quantum Dots: A New Class of Lasing Materials with Favorable Characteristics. *Advanced materials* **27,** 7101–7108, doi: 10.1002/adma.201503573 (2015).
12. Xu, Y. *et al.* Two-Photon-Pumped Perovskite Semiconductor Nanocrystal Lasers. *Journal of the American Chemical Society* **138,** 3761–3768, doi: 10.1021/jacs.5b12662 (2016).
13. Lu, Q. *et al.* The Role of Excitons on Light Amplification in Lead Halide Perovskites. *Advanced materials*, doi: 10.1002/adma.201603019 (2016).
14. Gu, Z. Y. *et al.* Two-Photon Pumped CH3NH3PbBr3 Perovskite Microwire Lasers. *Advanced Optical Materials* **4,** 472–479, doi: 10.1002/adom.201500597 (2016).
15. Yang, D. *et al.* Amplified Spontaneous Emission from Organic-Inorganic Hybrid Lead Iodide Perovskite Single Crystals under Direct Multiphoton Excitation. *Advanced Optical Materials* **4,** 1053–1059, doi: 10.1002/adom.201600047 (2016).
16. Yang, S. *et al.* Functionalization of perovskite thin films with moisture-tolerant molecules. *Nature Energy* **1,** 15016, doi: 10.1038/nenergy.2015.16 (2016).
17. Huang, H. *et al.* Water resistant CsPbX3nanocrystals coated with polyhedral oligomeric silsesquioxane and their use as solid state luminophores in all-perovskite white light-emitting devices. *Chem. Sci.* **7,** 5699–5703, doi: 10.1039/c6sc01758d (2016).
18. Swarnkar, A. *et al.* Quantum dot-induced phase stabilization of -CsPbI3 perovskite for high-efficiency photovoltaics. *Science* **354,** 92–95, doi: 10.1126/science.aag2700 (2016).
19. Wang, K. *et al.* Whispering-gallery-mode based CH3NH3PbBr3 perovskite microrod lasers with high quality factors. *Materials Chemistry Frontiers*, doi: 10.1039/C6QM00028B (2017).
20. Liao, Q. *et al.* Perovskite Microdisk Microlasers Self-Assembled from Solution. *Advanced materials* **27,** 3405–3410, doi: 10.1002/adma.201500449 (2015).
21. He, G. S., Bhawalkar, J. D., Prasad, P. N. & Reinhardt, B. A. Three-photon-absorption-induced fluorescence and optical limiting effects in an organic compound. *Optics letters* **20,** 1524–1526 (1995).
22. Yu, J. C. *et al.* Confinement of pyridinium hemicyanine dye within an anionic metal-organic framework for two-photon-pumped lasing. *Nature communications* **4,** doi: Artn 271910.1038/Ncomms3719 (2013).
23. Xing, G. *et al.* Low-temperature solution-processed wavelength-tunable perovskites for lasing. *Nature materials* **13,** 476–480, doi: 10.1038/nmat3911 (2014).
24. Zhu, H. *et al.* Lead halide perovskite nanowire lasers with low lasing thresholds and high quality factors. *Nature materials* **14,** 636–642, doi: 10.1038/nmat4271 (2015).
25. Liu, X. *et al.* Whispering gallery mode lasing from hexagonal shaped layered lead iodide crystals. *ACS nano* **9,** 687–695, doi: 10.1021/nn5061207 (2015).
26. Wang, K. *et al.* Formation of single-mode laser in transverse plane of perovskite microwire via micromanipulation. *Optics letters* **41,** 555–558, doi: 10.1364/OL.41.000555 (2016).
27. Wang, K. *et al.* High-Density and Uniform Lead Halide Perovskite Nanolaser Array on Silicon. *The journal of physical chemistry letters* **7,** 2549–2555, doi: 10.1021/acs.jpclett.6b01072 (2016).
28. Zhang, N. *et al.* Postsynthetic and Selective Control of Lead Halide Perovskite Microlasers. *The journal of physical chemistry letters* **7,** 3886–3891, doi: 10.1021/acs.jpclett.6b01751 (2016).
29. Wiersig, J. Hexagonal dielectric resonators and microcrystal lasers. *Physical Review A* **67,** 023807, doi: Artn 02380710.1103/Physreva.67.023807 (2003).
30. Wiersig, J. Formation of long-lived, scarlike modes near avoided resonance crossings in optical microcavities. *Physical review letters* **97,** 253901, doi: 10.1103/PhysRevLett.97.253901 (2006).
31. Song, Q. H. & Cao, H. Improving optical confinement in nanostructures via external mode coupling. *Physical review letters* **105,** 053902, doi: 10.1103/PhysRevLett.105.053902 (2010).

Acknowledgements

The author would like to thank the financial support from National Natural Science Foundation of China under the Grant No. 11374078, Shenzhen Fundamental research projects (JCYJ20160301154309393, JCYJ20160505175637639, JCYJ20160427183259083), Public platform for fabrication and detection of micro- & nano-sized aerospace devices, and Shenzhen engineering laboratory on onganic-inorganic perovskite devices.

Author Contributions

Yisheng Gao conducted the optical experiment and simulation. Shuai Wang, Can Huang, Ningbo Yi, and Kaiyang Wang took part in some parts of the experiment. Shumin Xiao and Qinghai Song proposed the idea and wrote the manuscript. All authors have given approval to the final version of the manuscript.

Additional Information

Supplementary information accompanies this paper at http://www.nature.com/srep

Competing Interests: The authors declare no competing financial interests.

How to cite this article: Gao, Y. *et al.* Room temperature three-photon pumped $CH_3NH_3PbBr_3$ perovskite microlasers. *Sci. Rep.* **7**, 45391; doi: 10.1038/srep45391 (2017).

Publisher's note: Springer Nature remains neutral with regard to jurisdictional claims in published maps and institutional affiliations.